Open access • Proceedings Article • DOI:10.1117/12.2009618

Wind Farm Power Maximization Based On A Cooperative Static Game Approach

Jinkyoo Park, Soon-Duck Kwon, Kincho H. Law

Institutions: Stanford University, Chonbuk National University

Published on: 10 Apr 2013 - Proceedings of SPIE (International Society for Optics and Photonics)

Topics: Wind power, Blade pitch, Wind speed, Power optimizer and Turbine

Wind Farm Power Maximization Based On A Cooperative Static Game Approach

Jinkyoo Park[a], Soonduck Kwon[b] and Kincho H. Law[a]

[a]Stanford University, Stanford, USA
[b]Chonbuk National University, Chunju-si, South Korea

ABSTRACT

The objective of this study is to improve the cost-effectiveness and production efficiency of wind farms using cooperative control. The key factors in determining the power production and the loading for a wind turbine are the nacelle yaw and blade pitch angles. However, the nacelle and blade angles may adjust the wake direction and intensity in a way that may adversely affect the performance of other wind turbines in the wind farm. Conventional wind-turbine control methods maximize the power production of a single turbine, but can lower the overall wind-farm power efficiency due to wake interference. This paper introduces a cooperative game concept to derive the power production of individual wind turbine so that the total wind-farm power efficiency is optimized. Based on a wake interaction model relating the yaw offset angles and the induction factors of wind turbines to the wind speeds experienced by the wind turbines, an optimization problem is formulated with the objective of maximizing the sum of the power production of a wind farm. A steepest descent algorithm is applied to find the optimal combination of yaw offset angles and the induction factors that increases the total wind farm power production. Numerical simulations show that the cooperative control strategy can increase the power productions in a wind farm.

Keywords: Wind Farm Control, Wake interference, Cooperative Control, Gradient Decent Method

1. INTRODUCTION

As concerns about greenhouse gas emissions and oil prices keep growing, renewable energy sources, such as wind power in particular, have received increased attention. According to the World Wind Energy Association (WWEA), at the end of 2011, the total energy generated by wind power worldwide had reached 239 GW, which is equivalent to 2.5% of the global electricity consumption.[1] As of 2012, wind turbines with a total capacity of 49 GW have been installed and have provided 120 TWh which is equivalent to 2.9% of all electric energy generated in the U.S..[2] The U.S. government has announced that wind energy will provide 20% of electricity needs by 2030.[2] To meet the target, not only the number of wind farms needs to increase, but the efficiency of power generation, especially in the wind farm scale, must also improve.

Researchers have striven to increase the performance of a wind turbine in terms of both the structural integrity and the power production. Control technologies have been implemented to reduce the load effects on a wind turbine,[3–6] and to increase the power efficiency.[7] Realizing the fact that the wind farm power efficiency can significantly degrade due to the wake interference among the wind turbines, researchers have recently started to study the efficiency of a wind farm as a whole rather than a single wind turbine. The optimum layout of wind turbines in a wind farm to minimize the wake interference under certain wind conditions (wind speed, direction, etc.) has been studied.[8,9] Studies on the coordination of the actions of the wind turbines to increase the wind farm power efficiency have also been reported. For example, many researchers have studied about how to find the optimum joint set of induction factors to account for the aerodynamic interactions among multiple wind turbines in a wind farm to maximize the total power output.[10,11] Machine learning algorithm has also been proposed to determine the optimum set of induction factors that can lead to efficiency increase in a wind farm under certain

Further author information:
Jinkyoo Park: E-mail: jkpark.11@stanford.edu
Soonduck Kwon: E-mail: sdkwon@chonbuk.ac.kr
Kincho H. Law: E-mail: law@stanford.edu

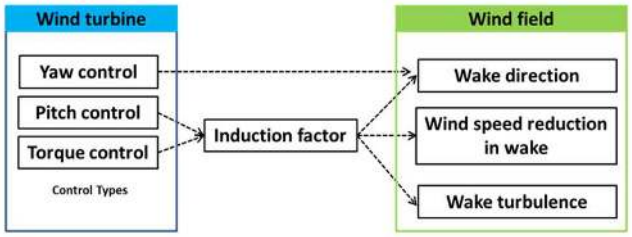

Figure 1: The relationshp between control actions of a wind turbine and the wind field.

wind directions.[12] Wind turbine yaw control mechanism has also been employed as a way to increase the power efficiency of wind farms.[13,14] However, a control strategy utilizing both the yaw offset angle and the induction factor as control variables has rarely been reported.

Maximizing the power of a wind farm can be posed as an optimization (control) problems. The main questions of the optimization problem include: (i) how to denote the optimization variables; (ii) how to formulate the problem; and (iii) how to determine the optimum solution? In this paper, we construct the problem as to maximize the total power production in a wind farm. We use yaw offset angles and induction factors of wind turbines in a wind farm as the control (optimization) variables, and formulate the power maximization problem in a cooperative static game framework. We then try to find the optimum yaw offset angles by applying the steepest descent method. The optimized wind farm power efficiencies corresponding to different wind directions are compared to the power efficiency of a wind farm obtained by conventional single-wind turbine control.

2. THEORETICAL BACKGROUND

2.1 Wind turbine control actions and wake

A wake can be defined as the region behind a wind turbine where, as compared to upstream wind flow, the wind speed is decreased and the turbulence is increased. A wake adversely affects the wind turbines in the downstream direction in two ways: i) it reduces the power production due to a decrease in the wind speed, and ii) it causes fatigue damage due to an increase in turbulence. Many researchers have studied the characteristics of wakes behind wind turbines.[15,16] The influence of wake on a real scale wind turbine can decrease the wind farm power efficiency up to 40 %.[17] As depicted in Fig. 1, yaw angle, blade pitch angle and rotor speed, which are designed for controlling a single wind turbine, can also affect the wind field in the wind farm by changing the characteristics of a wake (i.e., direction, turbulence level, and wind speed deficit ratio). The wind field modified by the wind turbines in the upstream influences the performance of the downstream wind turbines.

The control mechanisms take different time scales to activate. Because of the inertia of the rotor, changing the rotor direction (yaw control) can take significantly longer time than the other control actions on the blade pitch and the generator torque. It also takes a certain amount of time for a control action in the upstream wind turbine to influence the wake characteristics on the wind turbines in the downstream. Because of the complexity, this study consider only the mean wind field (steady state) to account for the wake interactions; accordingly, the time lag between the action and its influence is ignored.

2.1.1 The influence of induction factor on wake

The induction factor α is a measure of the retard in wind speed behind a wind turbine rotor and is defined as[18]

$$\alpha = \frac{U_\infty - U_{rotor}}{U_\infty} \tag{1}$$

where U_∞ and U_{rotor} are, respectively, wind velocities at the upstream and the rotor. The wind speed at the far downstream U_d is expressed as[18]

$$U_d = U_\infty(1 - 2\alpha) \tag{2}$$

Based on conservation of momentum, the power P extracted by an ideal wind turbine in the upstream can be written in terms of the induction factor α as:[18]

$$P = \frac{1}{2}\rho A U_\infty^3 4\alpha(1-\alpha)^2 = \frac{1}{2}\rho A U_\infty^3 C_P(\lambda, \beta) \tag{3}$$

where ρ and A are the air density and the rotor area, respectively. The term $C_P(\lambda, \beta)$ is the power coefficient representing the ratio of the power extracting from the wind fluid energy, which is a function of the rotor tip speed ratio λ (between the blade tip angular speed and the wind speed) and the blade pitch angle β. The power P is maximum when the induction factor α is $\frac{1}{3}$, which results in a downstream wind speed $U_d = U_\infty(1-2\times\frac{1}{3}) = \frac{1}{3}U_\infty$ as seen in Eq. 2. The induction factor can be adjusted by the blade pitch angle β and the rotor tip speed ratio λ. When accounting for the power production of the downstream wind turbines in an array, the induction factor of $\frac{1}{3}$ in the upstream wind turbine does not lead to the total maximum power output for the wind farm as a whole.[10] On the contrary, reducing the power extraction in the upstream wind turbine by adjusting the induction factor can potentially lead to an increase in the power production of the downstream wind turbines. This observation motivates shifting the individual-wind turbine based control paradigm to a cooperative, system-level control of wind turbines.

2.1.2 The influence of yaw offset angle on wake

Let's denote the yaw offset angle by x as the angle between the wind direction and the normal vector of a rotor surface as shown in Fig. 2a. The yaw offset angle can skew the wake direction, thus can possibly reduce wake interference and increase the power production in the other wind turbines.[19] With respect to individual wind turbine control, an increase of the yaw offset angle would reduce the power. However, as shown in Fig. 2b, the level of power reduction is relatively small when the yaw offset angle is less than 16 degrees. If the level of increases in the power from the downstream wind turbines due to the wake angle deflection exceeds the level of power decrease in the upstream wind turbine, the total wind farm power would increase. The relationship between the yaw offset angle x and the wake skew angle $\Delta\theta_{wake}$ has been studied by many researchers.[13,14] The following relationship has been obtained based on the measurements from a scaled wind farm:[14]

$$\Delta\theta_{wake} = 0.3 C_T x \tag{4}$$

The wake skew angle is related to the thrust coefficient C_T, which is the ratio of a thrust force to the aerodynamic force on a rotor of wind turbine. The thrust coefficient C_T ($C_T \approx 4\alpha(1-\alpha)$) is related to the induction factor α, which implies that the blade pitch angle β, which controls the induction factor α, can also influence the amount of wake deflection.[18] Prior study has shown that the wake skew angle can reduce the adverse effects on wind turbines in downstream flow and to increase the total power efficiency of wind turbines in a wind farm.[13,14] For example, wind tunnel simulation using 5 wind turbines with 250 mm rotor diameter has shown an 8.9 % increase in power output by controlling the wake skew angle.[13] The wake skewness by the yaw offset angle is verified in a scaled wind farm comprised of 10 wind turbines having rotor diameter of 7.6m and hub height of 7.5m.[14]

2.2 Wind farm power maximization in game theoretic framework

Game theory has successfully been used in modeling and analyzing how groups of people interact and derive their optimal strategies, especially in economics, politics, and sociology.[22] Due to its flexibility in formulating problems and its rigorous mathematical concepts, game theory has attracted interests from researchers in various engineering fields. Games can be divided into different categories based on how the agents' action evolve over time and how the agents interact. First, games can be categorized into static and dynamic games. In a static game, the agents choose their optimal actions for maximizing payoffs (or minimizing costs) in a single stage (i.e., single time step). In a dynamic game, however, the agents strive to maximize the sum of stage payoffs over the entire game period. Accordingly, agents need to account for the influence of current actions on their future payoffs. Because only the steady state wake interaction is considered in this study, a static game framework

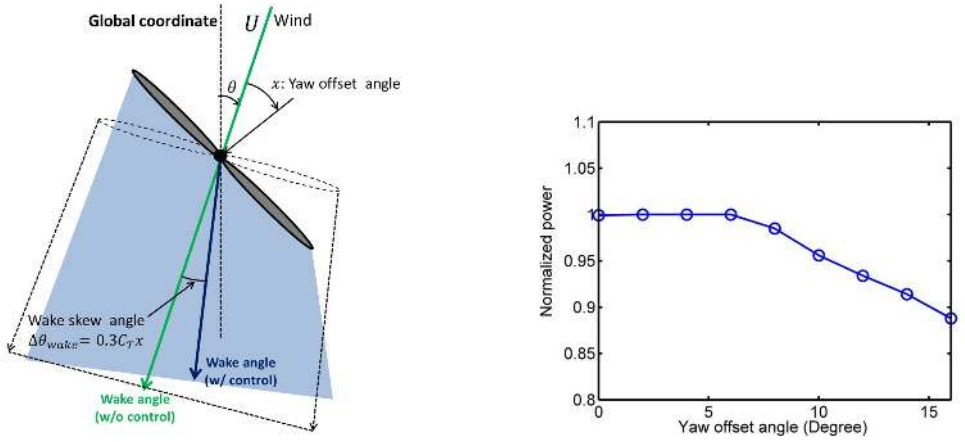

(a) Wake skewed angle (b) Influence of yaw offset angle on power

Figure 2: The influence of the yaw offset angle on the wake direction and power production: (a) shows the effect of the yaw offset angle on the wake direction, and (b) shows the power degradation with the increse in the yaw offset angle. The power output is simulated by using FAST,[20] an open-source wind turbine loads simulation code developed by the National Renewable Energy Laboratory (NREL), for a 5MW wind turbine model.[21]

is employed for deriving the optimal control actions among multiple wind turbines. Note that different wind conditions (i.e., different wind speeds and wind directions) would specify different static games, that for each game, an optimal control action needs to be derived. Games can also be categorized into non-cooperative and cooperative games according to the agents' behavior pattern. In a non-cooperative game, an agent seeks to optimize its own objective function without accounting for the other agents' cost. In a non-cooperative game, on the other hand, agents share the mutual objective function that all agents try to optimize in a cooperative manner. Because all the objective functions are converted into a single objective and agents are behaving as if they are one agent, the problem results in an optimization problem where the optimal actions by the agents optimize the common objective function.

2.2.1 Non-cooperative game

In a non-cooperative game, the Nash equilibrium is the core concept in deriving the optimal actions of multiple agents.[23] The control action s_i of the ith agent maximizing its objective function $f_i(\mathbf{s})$ which depends on the set of all control actions $\mathbf{s} = \{s_1, ..., s_N\}$ in a game. The Nash equilibrium $\mathbf{s}^* = \{s_1^*, ..., s_N^*\}$ satisfies the following relationship:

$$f_i(s_i^*, \mathbf{s}_{-i}^*) \geq f_i(s_i, \mathbf{s}_{-i}^*) \tag{5}$$

where $\mathbf{s}_{-i}$ is the complementary subset of $\mathbf{s}$ except s_i and $f_i(s_i, \mathbf{s_{-i}})$ is the objective function that the agent i tries to maximize over its own action s_i corresponding to the actions set $\mathbf{s_{-i}}$ of other agents. (Note that $\mathbf{s}_{-i}$ is a vector if the number of agents are greater than 2.) If all the agents except the agent i hold the Nash equilibrium actions $\mathbf{s}_{-i}^*$, the action of the agent i deviated from s_i^* will decrease its own objective function according to Eq. 5.

The independent control of a single wind turbine leads the wind turbines in a wind farm to produce power at the Nash equilibrium point. Denoting $\mathbf{x} = \{x_1, ..., x_N\}$ as the vector of the yaw offset angles and $\boldsymbol{\alpha} = \{\alpha_1, ..., \alpha_N\}$ as the vector of the induction factors of the wind turbines, in the example of this study, the ith wind turbine power (objective function) is expressed as

$$P_i(x_i, \alpha_i, \mathbf{x}_{-i}, \boldsymbol{\alpha}_{-i}) = \frac{1}{2}\rho A u_i^3(\mathbf{x}_{-i}, \boldsymbol{\alpha}_{-i})\cos^2(x_i)4\alpha_i(1-\alpha_i)^2 \tag{6}$$

where $u_i^3(\mathbf{x}_{-i}, \boldsymbol{\alpha}_{-i})$ is the wind speed experienced by ith wind turbine, which is influenced by the control actions $\{\mathbf{x}_{-i}, \boldsymbol{\alpha}_{-i}\}$ of other wind turbines. Empirically, the power degradation has been expressed in terms of the power of the cosine of the yaw offset angle, $\cos^\kappa(x_i)$ where $\kappa = 1.88$, as noted by Dahlberg.[13] In Eq. 6, for simplicity, the term $\cos^2(x_i)$ is used here as a means to capture the power degradation due to the yaw offset angle x_i.

As a non-cooperative game, the optimal pair of the yaw offset angle and the induction factor for each wind turbine can be found as

$$\begin{aligned}(x_i^*, \alpha_i^*) &= \arg\max_{x_i,\alpha_i} P_i(x_i, \alpha_i, \mathbf{x^*}_{-i}, \boldsymbol{\alpha^*}_{-i}) \\ &= \arg\max_{x_i,\alpha_i} \frac{1}{2}\rho A u_i^3(\mathbf{x}^*_{-i}, \boldsymbol{\alpha}^*_{-i})\cos^2(x_i)4\alpha_i(1-\alpha_i)^2, \qquad \text{for} \quad i = 1, ..., N \end{aligned} \tag{7}$$

Therefore, the Nash equilibrium point $\mathbf{x}^*$ and $\boldsymbol{\alpha}^*$ are obtained as

$$\mathbf{x}^* = \{x_i^*, \mathbf{x}^*_{-i}\} = \{x_i^*, ..., x_N^*\} = \{0, ..., 0\} \tag{8}$$

and

$$\boldsymbol{\alpha}^* = \{\alpha_i^*, \boldsymbol{\alpha}^*_{-i}\} = \{\alpha_i^*, ..., \alpha_N^*\} = \left\{\frac{1}{3}, ..., \frac{1}{3}\right\} \tag{9}$$

Since for any x_i and α_i

$$u_i^3(\mathbf{x}^*_{-i}, \boldsymbol{\alpha}^*_{-i})\cos^2(0)4\left(\frac{1}{3}\right)\left(1-\frac{1}{3}\right)^2 \geq u_i^3(\mathbf{x}^*_{-i}, \boldsymbol{\alpha}^*_{-i})\cos^2(x_i)4\alpha_i(1-\alpha_i)^2 \tag{10}$$

That is, the yaw offset angle x_i deviated from 0 and the induction factor α_i deviated from $\frac{1}{3}$ reduces ith wind turbine power only. Therefore, the conventional wind turbine control maximizing its own power by setting the rotor direction perpendicular to the wind direction (yaw offset angle = 0 degree) and extracting the most energy from wind flow (induction factor = $\frac{1}{3}$) reflects a Nash equilibrium point.

2.2.2 Cooperative game

In a cooperative game, all agents attempt to optimize cooperatively to achieve the common goal. The optimal control action $\mathbf{s}^*$ can be found by solving a multi-dimensional (vector) optimization problem defined as[22]

$$\mathbf{s}^*(\boldsymbol{\gamma}) = \arg\max_{\mathbf{s}\in\Re^N} \sum_{i=1}^{N} \gamma_i f_i(\mathbf{s}), \quad \gamma_i \geq 0 \tag{11}$$

where $\boldsymbol{\gamma} = \{\gamma_1, ..., \gamma_N\}$ is the vector consisting of the weighting coefficients on the objective function $f_i(\mathbf{s})$. Depending on $\boldsymbol{\gamma}$, different sets of Pareto solutions $f_i(\mathbf{s}^*(\boldsymbol{\gamma}))$ are obtained:

$$\{f_1(\mathbf{s}^*(\boldsymbol{\gamma})), ..., f_i(\mathbf{s}^*(\boldsymbol{\gamma})), ..., f_N(\mathbf{s}^*(\boldsymbol{\gamma}))\} \tag{12}$$

The fact that the actions in the upstream wind turbines can improve the power productions in the downstream wind turbines underscore the motivation of constructing wind farm power maximization problem in a cooperative game framework, which can be stated as

$$(\mathbf{x}^*, \boldsymbol{\alpha}^*) = \arg\max_{(\mathbf{x},\boldsymbol{\alpha})} \sum_{i=1}^{N} P_i(\mathbf{x}, \boldsymbol{\alpha}) = \arg\max_{(\mathbf{x},\boldsymbol{\alpha})} \sum_{i=1}^{N} \frac{1}{2}\rho A u_i^3(\mathbf{x}_{-i}, \boldsymbol{\alpha}_{-i})\cos^2(x_i)4\alpha_i(1-\alpha_i)^2 \tag{13}$$

where in this case we equally weight each wind turbine power (i.e.,$\gamma_i = 1$). In this wind farm power maximization setting, we seek to find the optimally coordinated sets of yaw offset angles $\mathbf{x}^*$ and induction factors $\boldsymbol{\alpha}^*$ that achieve the maximum total power. The static game for the steady state wake interaction and the cooperative game for the coordinated wind turbine control will be used as an analytical framework in this study.

3. FORMULATION

Denoting the yaw offset angles and the induction factors of wind turbines as the control variables, we formulate a wind farm power maximization problem in a cooperative static game framework. To establish a single objective function shared by all the wind turbines, we first need to construct the wake interaction model. The optimal control actions that maximize the objective function are then found by applying numerical optimization techniques. Therefore, the wind farm power maximization problem consists of two main parts: i) modeling the wake interaction by mapping the control actions to the wind speed experienced by the wind turbines in a wind farm, and ii) finding the optimum control actions of wind turbines that maximize the objective function, which, in this study, is assumed to be the sum of the power outputs from each wind turbine.

3.1 Wake model behind a single wind turbine

One of the most prevalent wake model is the Park wake model[24] that describes how the wind speed is retarded by the wake formed behind a wind turbine rotor. For a free stream wind speed U, the Park model defines the reduced wind speed u_i experienced by the ith wind turbine due to the wake formed behind the jth wind turbine in the upstream as[24]

$$u_i = (1 - \delta u(L^d, L^r, \alpha_j))U \tag{14}$$

where L^d and L^r are the wake distance in the downstream direction and the radial direction, respectively, as shown in Fig. 3. $\delta u(L^d, L^r, \alpha_j)$ is termed the wind speed deficit factor, which is a measure of the retarded wind speed and is given as:[24]

$$\delta u(L^d, L^r, \alpha_j) = \begin{cases} 2\alpha_j \left(\frac{D_j}{D_j + 2kL^d}\right)^2, & \text{if } L^r \leq \frac{D_j + 2kL^d}{2} \\ 0, & \text{otherwise} \end{cases} \tag{15}$$

where α_j is the induction factor of the jth wind turbine, D_j is the diameter of jth wind turbine, and k denotes the surface roughness. As seen in Eq. 15, the wake region is defined in the form of a 3D cone, whose diameter is $D_j + 2kL^d$, and the level of deficit factor is defined only in the inside of the wake. As L^d increases, the deficit factor decreases and the diameter of the wake expands.

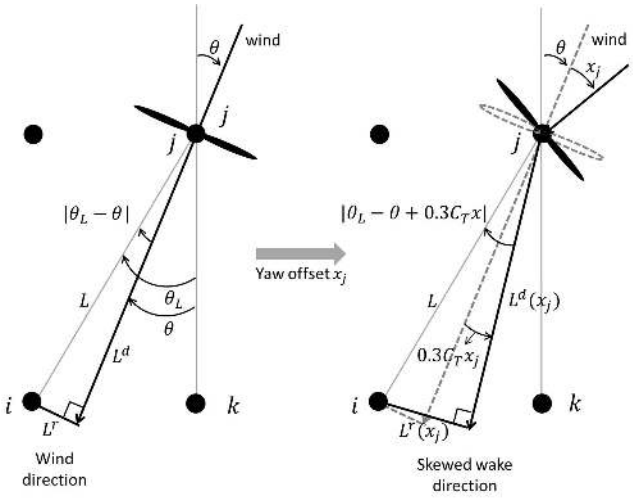

Figure 3: The influence of the yaw offset angle x_j on the wake direction and on the wake downstream distance L^d and the radial distance L^r. Note that the wind farm related parameters L and θ_L are subject to change with wind direction variation; for example, when wind direction θ is 0 degree, L is the interdistance to the alinged wind turbine k and the layout angle θ_L is zero.

As seen in Eq. 4, the yaw offset angle x_j can deflect the wake direction by $0.3C_T x_j$, which affects the wake distances L^d and L^r of the jth wind turbine as shown in Fig. 3. For the ith downstream wind turbine at the inter distance L and at the layout angle θ_L away from the jth upstream wind turbine, the L^d and L^r can be expressed as a function of x_j with respect to the wind direction θ as follows:

$$\begin{aligned} L^d(x_j;\theta) &= L\cos(|\theta_L - \theta + 0.3C_T x_j|) \\ L^r(x_j;\theta) &= L\sin(|\theta_L - \theta + 0.3C_T x_j|) \end{aligned} \tag{16}$$

The semi-colon symbol is used here to separate the variable x_j and the parameter θ of a function. L and θ_L are wind farm parameters, whose values change depending on wind direction. Depending on the wind direction, a "downstream" wind turbine may vary. For example, as shown in Fig. 3, the wind turbine k becomes a downstream wind turbine when the wind direction $\theta = 0$ degree. The difference between $\theta_L - \theta$ determines the deficit factor

that the downstream wind turbine experiences and the effectiveness of the control actions (the yaw offset and the induction factor) on reducing the deficit factor, and maximizing the wind speed u_i.

The boolean classification of a wake region as defined by δu in Eq. 15 shows an abrupt change of the deficit factor δu to be zero when $L^r(x_j) > \frac{D_j+2kL^d(x_j)}{2}$, which makes the wind farm power optimization problem using the yaw offset angle difficult to analyze. To overcome the discontinuity problem that δu abruptly changes to zero, we alter the wake model to allow a smooth transition between the wake and non-wake regions by using the Sigmoid and Gaussian functions as

$$\delta u(L^d, L^r, \alpha_j) = \left(\frac{2\alpha_j}{1+\exp\left(L^d/5D_j\right)}\right)\frac{1}{\sqrt{2\pi}(\sigma+\zeta L^d)}\exp\left(-\frac{(L^r/D_j)^2}{2(\sigma+\zeta L^d)^2}\right) \tag{17}$$

The first term in the bracket describes how the wind speed deficit factor decreases (i.e., wind speed is recovered) as L^d increases. The term in the form of a Gaussian function depicts the decreasing trend of the deficit factor with the radial distance L^r. The deficit factor is maximum at the center of the wake, but rapidly decreases as the radial distance L^r increases. The smooth transition between the wake and non-wake regions resembles wind tunnel results in the literature showing that the wind speed distribution over the radial axis follows an inverted Gaussian curve.[25] The standard deviation term in the Gaussian function $\sigma + \zeta L^d$ describes how the wake width expands as the downstream distance L^d increases, which is analogues to the term $D_j + 2kL^d$ in Eq. 15. The term σ determines the initial wake width right behind a rotor, and ζ controls the rate of expansion in the wake width with L^d.

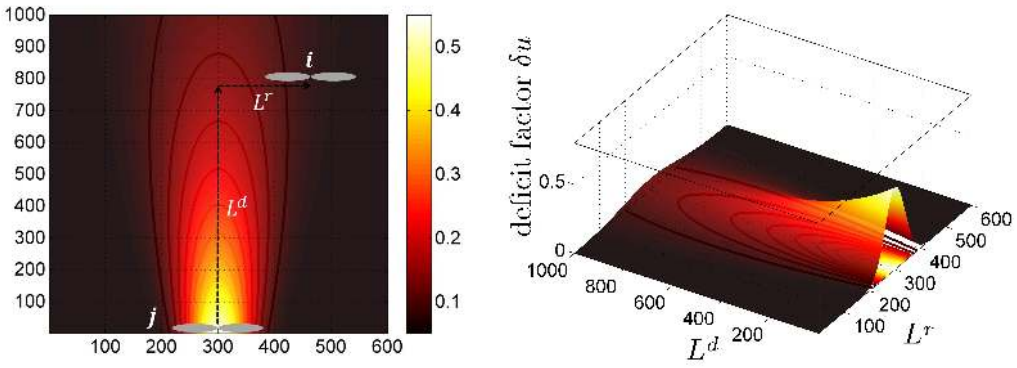

(a) Wind speed deficit factor

(b) Wind speed deficit factor (3D)

Figure 4: Wind speed deficit factor $\delta u(L_d, L_r, \alpha = 1/3)$ evaluted for every (L^d, L^r) grid point in the downstream direction

Fig. 4 shows the deficit factor evaluated at every grid point behind a wind turbine with a rotor diameter D_j of 140 m using Eq. 17. As shown in Fig. 4, the wake width expands with the wake downstream distance L^d (Fig. 4a), and the deficit factor decreases as L^d increases (Fig. 4b). Unlike the Park wake model that the wake and non-wake regions are abruptly separated, the wake region is smoothly and continuously defined over an infinite domain by Eq. 17. This feature facilitates the modeling of wake interactions among the wind turbine in a wind farm because now the wind speed experienced by the downstream wind turbine can be expressed in terms of a continuous and smooth function of x_j and α_j.

With the new wake deficit factor model (Eq. 17) and $L^d(x_j;\theta)$ and $L^r(x_j;\theta)$ (Eq. 16), we construct the deficit factor function $d(x_j, \alpha_j; \theta)$ relating the control actions, the yaw offset angle x_j and the induction factor α_i, in the upstream wind turbine j and the deficit factor δu at a downstream wind turbine j as follows:

$$d(x_j, \alpha_j; \theta) = \delta u(\mathrm{L}^d(x_j;\theta), L^r(x_j;\theta), \alpha_i) \tag{18}$$

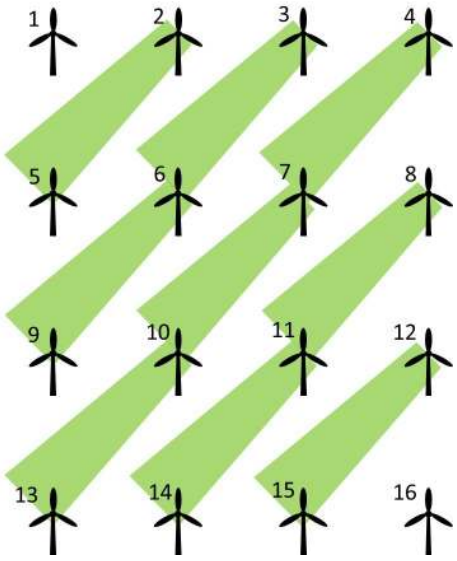

(a) Wake interference pattern in a wind farm ($\theta = 40°$)

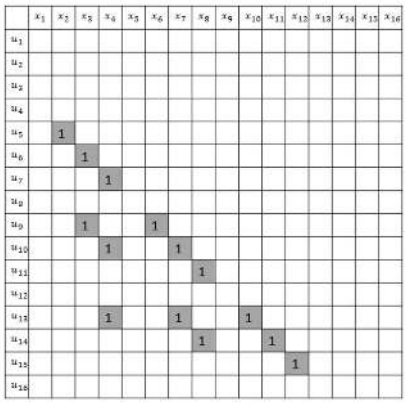

(b) Wake influencing matrix $W(\theta)$

Figure 5: Wake interactions among wind turbines in a wind farm: (a) shows how the wakes fromed by the upstream wind turbines affect the downstream wind turbines, and (b) shows the wake influecing matrix W that captures the wake interference patterns in a wind farm.

The wind speed u_i experienced by downstream wind turbine i given the free stream wind speed U and direction θ can be expressed in terms of control actions on the upstream wind turbine j as

$$u_i(x_j, \alpha_j; \theta, U) = (1 - d(x_j, \alpha_j; \theta))U \tag{19}$$

The wind speed experienced by a wind turbine and the corresponding power can now be expressed as a continuous and smooth function of the yaw offset angles and the induction factors.

3.2 Wake model behind multiple wind turbines

The wake formed behind an upstream wind turbine affects the downstream wind turbines, resembling a chain action. The retarded wind speed by the wake formed behind the upstream wind turbines serves as an input wind speed for the downstream wind turbine, while the wind speed retarding effects are being accumulated. Therefore the wind speed of the jth wind turbine is expressed in terms of the product of the marginal wind speed ratio (i.e., $1 - d$) over a chain of upstream wind turbines:

$$u_i(\mathbf{x}, \boldsymbol{\alpha}; \theta, U) = \left(\prod_{\{j|W(\theta)_{(i,j)}=1\}} (1 - d(x_j, \alpha_j; \theta)) \right) U \tag{20}$$

where $\mathbf{x}$=$(x_1, ..., x_N)$ and $\boldsymbol{\alpha}$=$(\alpha_1, ..., \alpha_N)$ denote, respectively, the set of yaw offset angles and the set of induction factors of N wind turbines in a wind farm. Similarly, $\mathbf{u} = \{u_1, ..., u_N\}$ denotes the wind speed experienced by each of the wind turbines.

We define a boolean wake influencing matrix $W(\theta)$, shown in Fig. 5b, describing how the wind turbines influence each other through the wake interference under the wind direction of θ. The $(i, j)^{th}$ entry of W is 1 if the wind turbine j influences the wind speed of the ith wind turbine, otherwise it is set to be zero. When $\theta = 40°$, as an example, the wind speed u_5, u_9, and u_{13} of the wind turbines 5, 9, and 13 as shown in Fig. 5a

can be expressed as follows:

$$u_5(\mathbf{x},\boldsymbol{\alpha};\theta,U) = (1-d(x_2,\alpha_2;\theta))\,U \tag{21}$$

$$u_9(\mathbf{x},\boldsymbol{\alpha};\theta,U) = (1-d(x_3,\alpha_3;\theta))\,(1-d(x_6,\alpha_6;\theta))\,U \tag{22}$$

$$u_{13}(\mathbf{x},\boldsymbol{\alpha};\theta,U) = (1-d(x_4,\alpha_4;\theta))\,(1-d(x_7,\alpha_7;\theta))\,(1-d(x_{10},\alpha_{10};\theta))\,U \tag{23}$$

Based on the relationships defined between the control actions from the wind turbines and the wind speeds experienced by the wind turbines in a wind farm, the power of the ith wind turbine (as shown in Eq. 3) can now be expressed as

$$P_i(\mathbf{x},\boldsymbol{\alpha};\theta,U) = \frac{1}{2}\rho A u_i^3(\mathbf{x},\boldsymbol{\alpha};\theta,U)\cos^2(x_i)4\alpha_i(1-\alpha_i)^2 \tag{24}$$

Note that the power of the ith wind turbine is influenced by not only its own yaw offset angle x_i and the induction factor α_i, but also the control actions, as represented by the vectors $\mathbf{x}$ and $\boldsymbol{\alpha}$, from the other wind turbines.

4. OPTIMIZATION PROCEDURE

Given a wind direction θ and a free stream wind speed $U(=U_\infty)$, the wind farm power maximization problem undertaken in this study, which is cast as a cooperative static game, is as follows:

$$\begin{aligned} \underset{\mathbf{x},\boldsymbol{\alpha}}{\text{maximize}} \quad & \sum_{i=1}^{N} P_i(\mathbf{x},\boldsymbol{\alpha};\theta,U) \\ \text{subject to} \quad & -\mathbf{x}_m \le \mathbf{x} \le \mathbf{x}_m \quad \text{and } \boldsymbol{\alpha}_l \le \boldsymbol{\alpha} \le \boldsymbol{\alpha}_u \end{aligned} \tag{25}$$

where -$\mathbf{x}_m$ and $\mathbf{x}_m$ denote, respectively, the minimum and the maximum allowable yaw offset angles, and $\boldsymbol{\alpha}_l$ and $\boldsymbol{\alpha}_u$ are, respectively, the lower and the upper bounds on the induction factors of wind turbines.

The wake interaction model mapping the yaw offset angles $\mathbf{x}$ and the induction factors $\boldsymbol{\alpha}$ of wind turbines to the wind speeds $\mathbf{u}$ experienced by the wind turbines is linearized. The linearized model can be effectively used to update the wake interaction model utilizing the measured input and output data $\{(\mathbf{x}^{(1)},\mathbf{u}^{(1)}),..,(\mathbf{x}^{(t)},\mathbf{u}^{(t)})\}$ in order to account for the uncertainties both in the wake model and the wind conditions in a wind farm. Based on the linearized model, the optimum joint sets of the yaw offset angles and the induction factors of wind turbines are found given different wind directions. The (optimized) power efficiencies obtained from the cooperative control strategy are compared with the case of greedy control where the yaw offset angles are set to zero and the induction factors are set as $\frac{1}{3}$ for all wind turbines in a wind farm.

4.1 A linear wake interaction model

The wake interaction model is linearized based on the first order Taylor's expansion as follows:

$$\mathbf{u}(\mathbf{x},\boldsymbol{\alpha};\theta,U) \approx \mathbf{u}\left(\mathbf{x_0},\boldsymbol{\alpha}_0;\theta,U\right) + J_{\mathbf{u}/\mathbf{x}}\left(\mathbf{x_0},\boldsymbol{\alpha}_0;\theta,U\right)\left(\mathbf{x}-\mathbf{x_0}\right) + J_{\mathbf{u}/\boldsymbol{\alpha}}\left(\mathbf{x_0},\boldsymbol{\alpha}_0;\theta,U\right)\left(\boldsymbol{\alpha}-\boldsymbol{\alpha}_0\right) \tag{26}$$

where $\mathbf{u}\left(\mathbf{x_0},\boldsymbol{\alpha}_0;\theta,U\right)$ is the vector denoting the wind speed experienced by the wind turbines when no yaw offset control($\mathbf{x_0}=\mathbf{0}$) and no induction factor control ($\boldsymbol{\alpha}_0=\frac{1}{3}\mathbf{1}$) are implemented. That is $\mathbf{u}\left(\mathbf{x_0},\boldsymbol{\alpha}_0;\theta,U\right)$ corresponds to the Nash equilibrium point. From Eq. 20, $u_i(\mathbf{0},\frac{1}{3}\mathbf{1};\theta,U) = \left(\prod_{\{j|W_{(i,j)}=1\}}\left(1-d(x_j,\alpha_j;\theta)\right)\right)U\Big|_{\mathbf{x_0}=\mathbf{0},\boldsymbol{\alpha}_0=\frac{1}{3}\mathbf{1}} = U\left(1-d(0,\frac{1}{3};\theta)\right)^{w_i^T\mathbf{1}}$, where w_i^T denotes the ith row of the matrix W and $\mathbf{1}$ is the unit vector. Therefore, the initial wind speed vector $\mathbf{u}\left(\mathbf{x_0},\boldsymbol{\alpha}_0;\theta,U\right)$ can be easily found by evaluating the deficit factor at x_j=0 and α_j=$\frac{1}{3}$. The Jacobian matrices $J_{\mathbf{u}/\mathbf{x}}\left(\mathbf{x_0},\boldsymbol{\alpha}_0;\theta,U\right)$ and $J_{\mathbf{u}/\boldsymbol{\alpha}}\left(\mathbf{x_0},\boldsymbol{\alpha}_0;\theta,U\right)$ denote, respectively, $\frac{\partial\mathbf{u}}{\partial\mathbf{x}}$ and $\frac{\partial\mathbf{u}}{\partial\mathbf{x}}$ evaluated at $\mathbf{x_0}=\mathbf{0}$ and $\boldsymbol{\alpha}_0=\frac{1}{3}\mathbf{1}$ for the given wind conditions θ and U. From Eq. 20, the $(i,j)^{th}$ entries of the $J_{\mathbf{u}/\mathbf{x}}\left(\mathbf{x_0},\boldsymbol{\alpha}_0;\theta,U\right)$ and $J_{\mathbf{u}/\boldsymbol{\alpha}}\left(\mathbf{x_0},\boldsymbol{\alpha}_0;\theta,U\right)$ can be expressed as:

$$\left.\frac{\partial u_i}{\partial x_j}\right|_{\mathbf{x}=\mathbf{0},\boldsymbol{\alpha}=\frac{1}{3}\mathbf{1}} = \begin{cases} -U\left.\frac{\partial d(x_j,\alpha_j;\theta)}{\partial x_j}\right|_{x_j=0,\alpha_j=\frac{1}{3}}(1-d(0,\frac{1}{3};\theta))^{(w_i^T\mathbf{1}-1)}, & \text{if } W_{i,j}(\theta)=1 \\ 0, & \text{otherwise} \end{cases} \tag{27}$$

$$\left.\frac{\partial u_i}{\partial \alpha_j}\right|_{\mathbf{x}=\mathbf{0},\boldsymbol{\alpha}=\frac{1}{3}\mathbf{1}} = \begin{cases} -U\left.\frac{\partial d(x_j,\alpha_j;\theta)}{\partial x_j}\right|_{x_j=0,\alpha_j=\frac{1}{3}} (1-d(0,\frac{1}{3};\theta))^{(w_i^T\mathbf{1}-1)}, & \text{if } W_{i,j}(\theta)=1 \\ 0, & \text{otherwise} \end{cases} \tag{28}$$

The term $(w_i^T\mathbf{1}-1)$ denotes the number of wind turbines that influence the ith wind turbine in a wind farm. In addition, from Eq. 16, $\frac{\partial d(x_j,\alpha_j;\theta)}{\partial x_j}$ can be obtained by applying the chain rule as follows:

$$\frac{\partial d(x_j,\alpha_j;\theta)}{\partial x_j} = \frac{\partial \delta u(L^d,L^r,\alpha_j)}{\partial L^d}\frac{\partial L^d(x_j;\theta)}{\partial x_j} + \frac{\partial \delta u(L^d,L^r,\alpha_j)}{\partial L^r}\frac{\partial L^r(x_j;\theta)}{\partial x_j} \tag{29}$$

To illustrate, evaluating $\frac{\partial u_5}{\partial x_2}$, $\frac{\partial u_9}{\partial x_3}$, and $\frac{\partial u_{13}}{\partial x_4}$ at $\mathbf{x}=\mathbf{0}$ and $\boldsymbol{\alpha}=\frac{1}{3}\mathbf{1}$ gives

$$\begin{aligned}
\left.\frac{\partial u_5}{\partial x_2}\right|_{\mathbf{x}=\mathbf{0},\boldsymbol{\alpha}=\frac{1}{3}\mathbf{1}} &= -U\left.\frac{\partial d(x_2,\alpha_2;\theta)}{\partial x_2}\right|_{\mathbf{x}=\mathbf{0},\boldsymbol{\alpha}=\frac{1}{3}\mathbf{1}} = -U\epsilon_x' \\
\left.\frac{\partial u_9}{\partial x_3}\right|_{\mathbf{x}=\mathbf{0},\boldsymbol{\alpha}=\frac{1}{3}\mathbf{1}} &= -U\left.\frac{\partial d(x_3,\alpha_3;\theta)}{\partial x_3}(1-d(x_6,\alpha_6;\theta))\right|_{\mathbf{x}=\mathbf{0},\boldsymbol{\alpha}=\frac{1}{3}\mathbf{1}} = -U\epsilon_x'(1-\epsilon) \\
\left.\frac{\partial u_{13}}{\partial x_4}\right|_{\mathbf{x}=\mathbf{0},\boldsymbol{\alpha}=\frac{1}{3}\mathbf{1}} &= -U\left.\frac{\partial d(x_4,\alpha_4;\theta)}{\partial x_4}(1-d(x_7,\alpha_7;\theta))(1-d(x_{10},\alpha_{10};\theta))\right|_{\mathbf{x}=\mathbf{0},\boldsymbol{\alpha}=\frac{1}{3}\mathbf{1}} = -U\epsilon_x'(1-\epsilon)^2
\end{aligned} \tag{30}$$

where $\epsilon_x' = \left.\frac{\partial d(x_j,\alpha_j;\theta)}{\partial x_j}\right|_{x_j=0,\alpha_j=\frac{1}{3}}$ and $\epsilon = d(0,\frac{1}{3};\theta)$. Similarly, evaluating $\frac{\partial u_5}{\partial \alpha_2}$, $\frac{\partial u_9}{\partial \alpha_3}$, and $\frac{\partial u_{13}}{\partial \alpha_4}$ at $\mathbf{x}=\mathbf{0}$ and $\boldsymbol{\alpha}=\frac{1}{3}\mathbf{1}$ gives

$$\begin{aligned}
\left.\frac{\partial u_5}{\partial \alpha_2}\right|_{\mathbf{x}=\mathbf{0},\boldsymbol{\alpha}=\frac{1}{3}\mathbf{1}} &= -U\left.\frac{\partial d(x_2,\alpha_2;\theta)}{\partial \alpha_2}\right|_{\mathbf{x}=\mathbf{0},\boldsymbol{\alpha}=\frac{1}{3}\mathbf{1}} = -U\epsilon_\alpha' \\
\left.\frac{\partial u_9}{\partial \alpha_3}\right|_{\mathbf{x}=\mathbf{0},\boldsymbol{\alpha}=\frac{1}{3}\mathbf{1}} &= -U\left.\frac{\partial d(x_3,\alpha_3;\theta)}{\partial \alpha_3}(1-d(x_6,\alpha_6;\theta))\right|_{\mathbf{x}=\mathbf{0},\boldsymbol{\alpha}=\frac{1}{3}\mathbf{1}} = -U\epsilon_\alpha'(1-\epsilon) \\
\left.\frac{\partial u_{13}}{\partial \alpha_4}\right|_{\mathbf{x}=\mathbf{0},\boldsymbol{\alpha}=\frac{1}{3}\mathbf{1}} &= -U\left.\frac{\partial d(x_4,\alpha_4;\theta)}{\partial \alpha_4}(1-d(x_7,\alpha_7;\theta))(1-d(x_{10},\alpha_{10};\theta))\right|_{\mathbf{x}=\mathbf{0},\boldsymbol{\alpha}=\frac{1}{3}\mathbf{1}} = -U\epsilon_\alpha'(1-\epsilon)^2
\end{aligned} \tag{31}$$

where $\epsilon_\alpha' = \left.\frac{\partial d(x_j,\alpha_j;\theta)}{\partial \alpha_j}\right|_{x_j=0,\alpha_j=\frac{1}{3}}$

It is interesting to note that the non-zero components in the same row of the two Jacobian matrices, $J_{\mathbf{u}/\mathbf{x}}$ and $J_{\mathbf{u}/\boldsymbol{\alpha}}$, evaluated at $\mathbf{x}=\mathbf{0}$ and $\boldsymbol{\alpha}=\frac{1}{3}\mathbf{1}$ are all identical. Furthermore, the sparsity patterns of $J_{\mathbf{u}/\mathbf{x}}(\mathbf{x_0},\boldsymbol{\alpha}_0;\theta,U)$ and $J_{\mathbf{u}/\boldsymbol{\alpha}}(\mathbf{x_0},\boldsymbol{\alpha}_0;\theta,U)$ are the same as the sparsity pattern of the wake influencing matrix $W(\theta)$. Corresponding to the 4×4 wind turbine array and the wind direction $\theta=40^\circ$ as shown in Fig. 5a, the Jacobian matrix $J_{\mathbf{u}/\mathbf{x}}(\mathbf{x_0},\boldsymbol{\alpha}_0;\theta,U)$ can be represented as

$$J_{\mathbf{u}/\mathbf{x}}(\theta,U) = -U\begin{bmatrix}
0 & 0 & 0 & 0 & 0 & 0 & 0 & 0 & 0 & 0 & 0 & 0 & 0 & 0 & 0 & 0 \\
0 & 0 & 0 & 0 & 0 & 0 & 0 & 0 & 0 & 0 & 0 & 0 & 0 & 0 & 0 & 0 \\
0 & 0 & 0 & 0 & 0 & 0 & 0 & 0 & 0 & 0 & 0 & 0 & 0 & 0 & 0 & 0 \\
0 & 0 & 0 & 0 & 0 & 0 & 0 & 0 & 0 & 0 & 0 & 0 & 0 & 0 & 0 & 0 \\
0 & \epsilon' & 0 & 0 & 0 & 0 & 0 & 0 & 0 & 0 & 0 & 0 & 0 & 0 & 0 & 0 \\
0 & 0 & \epsilon' & 0 & 0 & 0 & 0 & 0 & 0 & 0 & 0 & 0 & 0 & 0 & 0 & 0 \\
0 & 0 & 0 & \epsilon' & 0 & 0 & 0 & 0 & 0 & 0 & 0 & 0 & 0 & 0 & 0 & 0 \\
0 & 0 & 0 & 0 & 0 & 0 & 0 & 0 & 0 & 0 & 0 & 0 & 0 & 0 & 0 & 0 \\
0 & 0 & \epsilon'(1-\epsilon) & 0 & 0 & \epsilon'(1-\epsilon) & 0 & 0 & 0 & 0 & 0 & 0 & 0 & 0 & 0 & 0 \\
0 & 0 & 0 & \epsilon'(1-\epsilon) & 0 & 0 & \epsilon'(1-\epsilon) & 0 & 0 & 0 & 0 & 0 & 0 & 0 & 0 & 0 \\
0 & 0 & 0 & 0 & 0 & 0 & 0 & \epsilon' & 0 & 0 & 0 & 0 & 0 & 0 & 0 & 0 \\
0 & 0 & 0 & 0 & 0 & 0 & 0 & 0 & 0 & 0 & 0 & 0 & 0 & 0 & 0 & 0 \\
0 & 0 & 0 & \epsilon'(1-\epsilon)^2 & 0 & 0 & \epsilon'(1-\epsilon)^2 & 0 & 0 & \epsilon'(1-\epsilon)^2 & 0 & 0 & 0 & 0 & 0 & 0 \\
0 & 0 & 0 & 0 & 0 & 0 & 0 & \epsilon'(1-\epsilon) & 0 & 0 & \epsilon'(1-\epsilon) & 0 & 0 & 0 & 0 & 0 \\
0 & 0 & 0 & 0 & 0 & 0 & 0 & 0 & 0 & 0 & 0 & \epsilon' & 0 & 0 & 0 & 0 \\
0 & 0 & 0 & 0 & 0 & 0 & 0 & 0 & 0 & 0 & 0 & 0 & 0 & 0 & 0 & 0
\end{bmatrix} \tag{32}$$

The Jacobian matrix $J_{\mathbf{u}/\boldsymbol{\alpha}}(\mathbf{x_0},\boldsymbol{\alpha}_0;\theta,U)$ can be found similarly. Since we only evaluate the Jacobian matrices at the $\mathbf{x_0}$ and $\boldsymbol{\alpha}_0$, we denote $J_{\mathbf{u}/\mathbf{x}}(\mathbf{x_0},\boldsymbol{\alpha}_0;\theta,U)$ and $J_{\mathbf{u}/\alpha}(\mathbf{x_0},\boldsymbol{\alpha}_0;\theta,U)$ as $J_{\mathbf{u}/\mathbf{x}}(\theta,U)$ and $J_{\mathbf{u}/\alpha}(\theta,U)$, respectively, and express $\mathbf{u}(\mathbf{x},\boldsymbol{\alpha};\theta,U) \approx \mathbf{u}(\mathbf{x_0},\boldsymbol{\alpha}_0;\theta,U) + J_{\mathbf{u}/\mathbf{x}}(\theta,U)(\mathbf{x}-\mathbf{x_0}) + J_{\mathbf{u}/\boldsymbol{\alpha}}(\theta,U)(\boldsymbol{\alpha}-\boldsymbol{\alpha}_0)$. Now the linearized $u_i(\mathbf{x},\boldsymbol{\alpha};\theta,U)$ can be inserted into the wind farm power maximization problem, as stated in Eqs. 20 and 25.

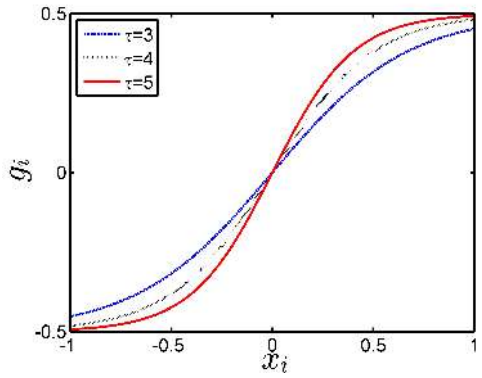

Figure 6: $g_i(x_i)$ function mapping the yaw offset angle x_i of ith wind turbine to the bounded value g_i. This paper uses $\tau = 4$ that gives a close approximiation of $g_i \approx x_i$ around 0.

4.2 Constraints on the yaw offset angles

As noted in Eq. 25, the range of $\mathbf{x}$ is constrained to the physically allowable yaw offset angles. In this study, we simplify the constraint by replacing $\mathbf{x}$ by a vector valued function $g(\mathbf{x})$, defined in a Sigmoid function form, whose ith component maps the control of jth wind turbine x_j to the bounded values. In this study, the yaw offset angles are limited between -0.5 to 0.5 radian and $g_j(x_j)$ is defined as

$$g_j(x_j) = 0.5\left(\frac{1-\exp(-\tau x_j)}{1+\exp(-\tau x_j)}\right) \tag{33}$$

where τ is the coefficient controlling the increasing rate of $g_j(x_j)$ with respect to that of yaw offset angle x_j. The relationship between x_j and $g_j(x_j)$ is shown in Fig. 6 with different values of τ. As shown in Fig. 6, when the yaw offset angle is between -0.5 and 0.5 (radians), the relationships between g_j and x_j is almost linear. When x_j exceeds 0.5, the function g_j asymptotically converges to its upper limit 0.5, in which there is no incentive for x_j to keep increasing because the excessive yaw offset angle x_j only reduces the power of jth wind turbine by $\cos^2(x_j)$ without increasing any wind speed. Replacing $\mathbf{x}$ with $g(\mathbf{x})$ prohibits the term $\cos(x_j)$ from changing its sign and preserve the concavity of the objective function, which guarantees the existence of the maximum in the objective function. Using the constructed linear wake interaction model, the power of the jth wind turbine can now be approximated as follows:

$$P_j(\mathbf{x},\boldsymbol{\alpha};\theta,U) \approx \frac{1}{2}\rho A\left(u_j(\mathbf{0},\frac{1}{3}\mathbf{1};\theta,U) + \{J_{\mathbf{u}/\mathbf{x}}(\theta,U)\}_j g(\mathbf{x}) + \{J_{\mathbf{u}/\alpha}(\theta,U)\}_j(\boldsymbol{\alpha}-\frac{1}{3}\mathbf{1})\right)^3 \cos^2(x_j)4\alpha_i(1-\alpha_j)^2 \tag{34}$$

where $\{J_{\mathbf{u}/\mathbf{x}}(\theta,U)\}_j$ and $\{J_{\mathbf{u}/\boldsymbol{\alpha}}(\theta,U)\}_j$ represents the jth row vector in the Jacobian matrices. The optimal control actions will be found using Eq. 34 to compute the approximated power output.

5. NUMERICAL SIMULATIONS

The joint sets of the optimal yaw offset angles $\mathbf{x}^*$ and the induction factors $\boldsymbol{\alpha}^*$ of 16 wind turbines in a wind farm arranged as shown in Fig. 5a are computed by optimizing the power output function in Eq. 25 using the steepest descent method.[26] Since the optimum control actions vary with wind directions, we solve the power maximization problem of Eq. 25 for wind directions varying from 0 to 90 degrees. We compare the greedy control and the cooperative control schemes in terms of the wind farm power efficiency defined as

$$\eta^*(\theta,U) = \frac{\sum_{i=1}^N \frac{1}{2}\rho A u_i^3(\mathbf{x}^*,\boldsymbol{\alpha}^*;U,\theta)\cos^2(x_i^*)4\alpha_i^*(1-\alpha_i^*)^2}{\sum_{i=1}^N \frac{1}{2}\rho A U^3\cos^2(0)4\left(\frac{1}{3}\right)\left(1-\frac{1}{3}\right)^2} \tag{35}$$

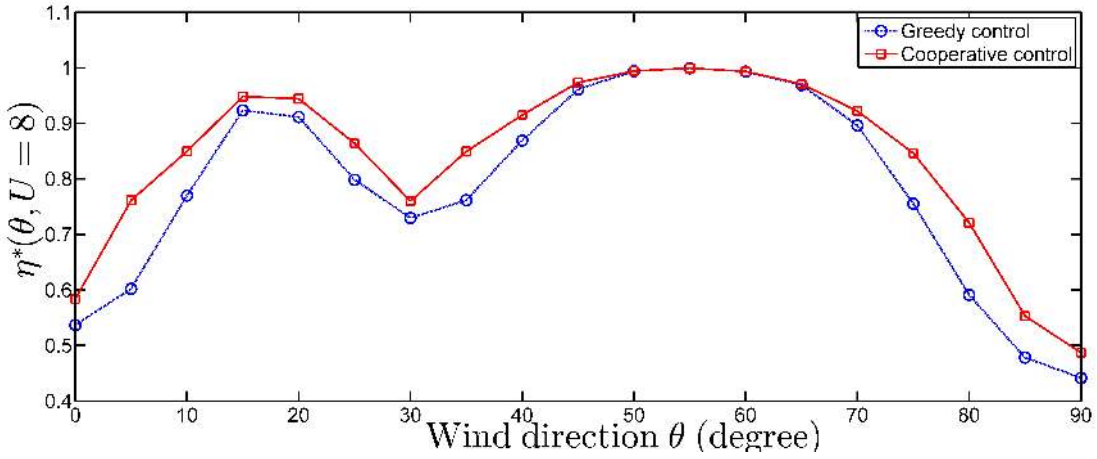

Figure 7: The wind farm power efficienty comparison between the greedy and cooperative control cases for diffent wind speeds; for the greedy control simulation, all the yaw offset angles and the induction factors for wind turbines are set to be 0 and $\frac{1}{3}$, respectively.

which denotes the the ratio between the power production in a wind farm and the maximum potential wind energy that can be extracted by the wind turbines if there are no wake interferences. Note that the optimal control actions $\mathbf{x}^*$ and $\boldsymbol{\alpha}^*$ are found based on the linearized wake interaction model (Eq. 26), but the efficiency $\eta^*(U, \theta)$ is evaluated using the non-linear model (Eq. 20).

Fig. 7 compares the maximized total wind farm power efficiency $\eta^*(\theta, U)$ with the wind farm power efficiency of the non-cooperative-greedy control. For the 4×4 wind turbines layout, the wind farm power efficiency for the greedy control case significantly drops when the wind direction aligns with the wind turbine array at $\theta = 0°$, $30°$ and $90°$, in which $|\theta - \theta_L|$=0. When the cooperative control is implemented, however, the degradation in the power efficiency is reduced except when the wind direction ($\theta \approx 55°$) does not cause wake interference among the wind turbines in a wind farm. That is, when $\theta \approx 55°$, wake formed by wind turbines in the upstream does not interfere the wind turbines in the downstream because the centerline of a wake is located in the middle of two wind turbines. In this case, any control actions of a wind turbine only induces the power degradation in its own power without making favorable wind to the downstream wind turbines.

We investigate how a wind turbine executes the control actions, yaw angle and induction factor adjustments, depending on its relative locations and wind directions. Fig. 8 shows the trends of the power, the yaw offset angle, and the induction factor of each individual wind turbine affected by the varying wind directions. Generally, the amount of the adjustments in the yaw offset angle and the induction factor in the upstream wind turbines are larger than those in the downstream wind turbines. For example, the optimized values of the yaw offset angle and the induction factor for the wind turbine 4 fluctuate depending on the wind directions. On the other hand, as shown in Fig. 8d, for the wind turbine 13 in the far downstream direction, the yaw offset angle and the induction factor are held as 0 and $\frac{1}{3}$, respectively. As shown in Figs. 8b to 8d, the power output increases when the cooperative efforts from wind turbines are carried out in the upstream.

From the observations in Fig. 8, the control actions can be categorized into three cases. First, when there are no wake interference among wind turbines (i.e., $50° \leq \theta \leq 65°$), both the yaw and the induction factor controls are not activated. Second, when the wind direction is aligned to the wind turbine array (i.e., $\theta = 0°$, $30°$ and $90°$) where wind turbines are completely overlaid by wakes formed behind the upstream wind turbines, the induction factor control is activated while the yaw angle is rarely offset. This is because a moderate yaw offset angle cannot reduce the wake interference, but changes in the induction factor can effectively minimize the wake interference. Finally, for other wind directions, the yaw offset angle and the induction factor controls are activated in an optimally coordinated manner to increase the total power. The three categories can be identified by comparing the relative magnitude of the norm for $\{J_{\mathbf{u}/\mathbf{x}}(\theta, U)\}_i$ and $\{J_{\mathbf{u}/\boldsymbol{\alpha}}(\theta, U)\}_i$ in Eq. 34.

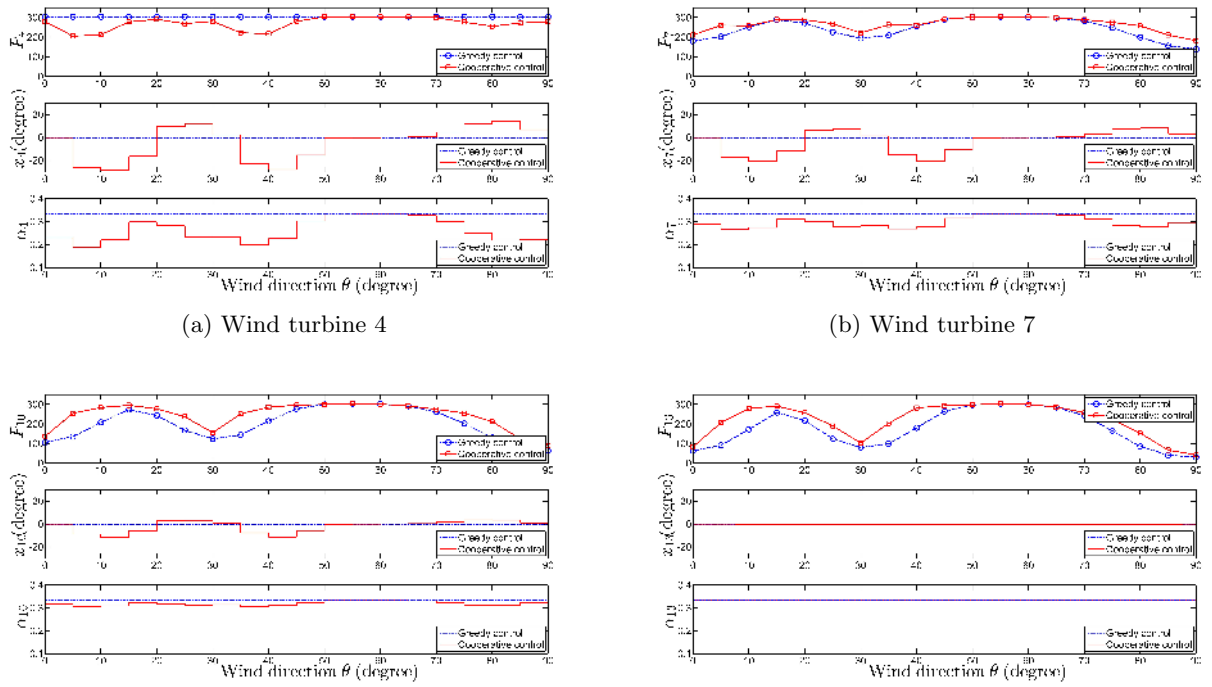

(a) Wind turbine 4

(b) Wind turbine 7

(c) Wind turbine 10

(d) Wind turbine 13

Figure 8: Comparison of the individual wind turbine power, yaw offsets, and induction factors between the greedy control (shown in dotted lines) and the cooperative control (swon in solid lines) for different wind speeds.

Fig. 9 compares the power in each individual wind turbine obtained using the non-cooperative greedy strategy and the cooperative strategy. The patterns of the power distribution among the wind turbines vary with the wind directions. For the non-cooperative greedy strategy, the upstream wind turbines hold its maximum power production under all wind directions, but a significant degradation of powers is observed in the downstream wind turbines. The non-cooperative strategy results in a greater level of disparity in the power productions from the wind turbines in a wind farm. When the cooperative control is implemented, as seen in Fig. 9, the upstream wind turbines (i.e., wind turbines 1, 2, 3, and 4 in Fig. 5a) yield only a fraction of the power, but the power productions in the downstream wind turbines increase.

6. SUMMARY AND DISCUSSIONS

This study examines the wind farm power maximization problem posed as a cooperative static game. The wake model describing the wind speed reduction behind a upstream wind turbine is modeled using a smooth and continuous function in the form of a Gaussian function and a Sigmoid function. The study then establishes the relationship between the control actions (i.e., adjustments of the yaw offset angle and the induction factor) of wind turbines and the wind speeds experienced by wind turbines in a wind farm. We linearize the relationship between the actions and the wind speeds and use the linearized model to construct the wind farm power maximization problem. Using the linearized model, the formulation of optimization problems corresponding to different wind conditions can be solved efficiently and systematically.

The steepest descent method is employed to compute the optimal joint sets of yaw offset angles and the induction factors that maximize the total wind farm power. For different wind directions, the cooperative control strategy that combines the yaw offset angle control and the induction factor control increases the wind farm power efficiency. Furthermore, the cooperative control strategy reduces the imbalance in the produced

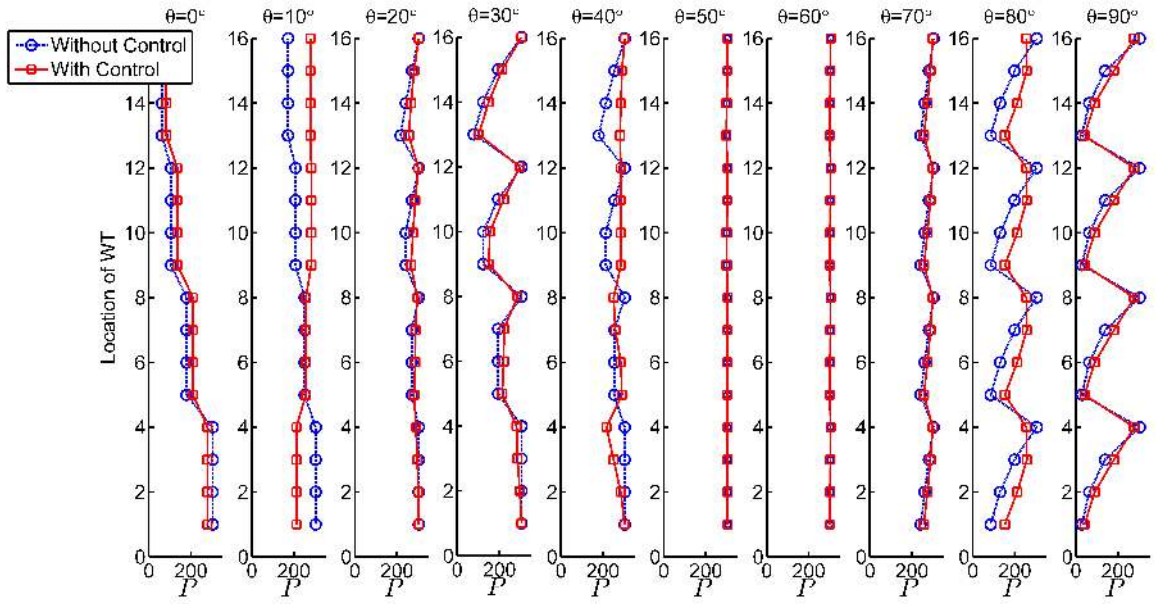

Figure 9: Power distribution over the wind turbines in a wind farm showing the wind turbine powers are localized mostly in the upstream wind turbines. The cooperative control reduce the power disparity among wind turbines in a wind farm.

powers from the wind turbines in a wind farm and thus seeks to equally redistribute the wind energy production to each wind.

In future work, the online updating of Jacobian matrices by using continuously measured actions and responses (i.e., wind speeds or power outputs from wind turbines) data will be integrated. To find the optimal control actions, distributed optimization method on the basis of the dual decomposition which can potentially improve the performance of numerical optimization by restricting the communication of information only among the neighboring wind turbines will be investigated.

ACKNOWLEDGMENTS

This research is partially supported by the US National Science Foundation under Grant No. CMMI-0824977. Any opinions, findings, and conclusions or recommendations expressed in this paper are those of the authors and do not necessarily reflect the views of the National Science Foundation.

REFERENCES

[1] Gsanger, S. and Pitteloud, J. D., [*World Wind Energy Report 2011*], World Wind Energy Association, Bonn, Germany (2012).

[2] Sutherland, H. J., [*U.S. Department of Energy Workshop Report: Reserach Needs for Wind Resource Characterization*], NREL/TP-500-43521, National Renewable Energy Laboratory, Golden, Co (2008).

[3] Johnson, S., van Dam, C., and Berg, D., [*Active Load Control Techniques for Wind Turbines*], SAND2008-4809, Sandia National Laboratories, Albuquerque, NM (2008).

[4] Bossanyi, E., "Wind turbine control for load reduction," *Wind Energy* **6**, 229–244 (2003).

[5] Saltoni, M., Wisniewski, R., Brath, P., and Boyd, S., "Load reduction of wind turbines using receding horizon control," *Proc. IEEE Multi-Conference on Systems and Control*, 852–857 (2011).

[6] Biegel, B., Juelsgaard, M., Kraning, M., Boyd, S., and Stoustrup, J., "Wind turbine pitch optimization," *Proc. IEEE Multi-conference on Systems and Control*, 1327–1334 (2011).

[7] Schaak, P., [*Heat and Flux : Enabling the Wind Turbine Controller*], ECN-E-06-017, Energy Eeseach Centre of the Netherlands (2006).

[8] Chowdhury, S., Zhang, J., Messac, A., and Castillo, L., "Unrestricted wind farm layout optimization (UWFLO): Investigating key factors influencing the maximum power generation," *Renewable Energy* **38**, 16–30 (2012).

[9] Kusiak, A. and Song, Z., "Design of wind farm layout for maximum wind energy capture," *Renewable Energy* **35**, 685–694 (2010).

[10] Johnson, K. and Thomas, N., "Wind farm control: addressing the aerodynamic interaction among wind turbines," *Proc. American Control Conference*, 2104–2109 (2009).

[11] Madjidian, D. and Ranter, A., "A stationary turbine interaction model for control wind farms," *Proc. 18th World Congress of the International Federation of Automatic Control* (2011). Available: http://www.control.lth.se/documents/2011/dar+ran11ifac.pdf (accessed 15th Fabuary 2013).

[12] Marden, J., Ruben, S., and Pao, L., "A model-free approach to wind farm control using game theoretic methdos," *IEEE Transactions on Control Systems Technology* (2013). Available: http://ecee.colorado.edu/marden/files/WF_Optimization.pdf (accessed 15th Fabuary 2013).

[13] Dahlberg, J. and Medici, D., "Potential improvement of wind turbine array efficiency by active wake control," *Proc. European Wind Energy Conference*, 65–84 (2003).

[14] Wagenaar, J., Machielse, L., and Schepers, J., "Controlling wind in ECN's scaled wind farm," *Proc. Europe Premier Wind Energy Event*, 685–694 (2012).

[15] Vermeer, L., "Wind turbine wake aerodynamics," *Progress in Aerospace Science* **39**, 467–510 (2003).

[16] Yang, Z., Sarkar, P., and Hu, H., "An experimental investigation on the wake characteristics of a wind turbine in an atmospheric boundary layer wind," *AIAA 2001-3815, Proc. 29th AIAA Applied Aerodynamics Conference* (2001).

[17] Mechali, M., Barthelmie, R., Frandsen, S., and Jensen, L., "Wake effects at Horns Rev and their influences on energy production," *Proc. European Wind Energy Conference and Exhibition* (2006). Available: http://johnstonanalytics.com/yahoo_site_admin/assets/docs/WakeEffectsWindTurbines.21172331.pdf (accessed 15th Fabuary 2013).

[18] Manwell, J. F., McGowan, J. G., and Rogers, A. L., [*Wind Energy Explained: Theory, Design and Application*], John Wiley & Sons (2002).

[19] Medici, D., [*Wind Turbine Wakes - Control and Vortex Shedding*], S-100 44, Royal Institute of Technology, Stockholm, Sweden (2004).

[20] Jonkman, J. M. and Buhl, M. L., [*FAST User's Guide*], NREL/EL-500-38230, National Renewable Energy Laboratory, Golden, Co (2005).

[21] Jonkman, J. M., Butterfield, S., Musical, W., and Scott, G., [*Definition of a 5MW Reference Wind Turbine for an offshore System Development*], NREL/TP-500-38060, National Renewable Energy Laboratory, Golden, Co (2007).

[22] Engwerda, J. C., [*LQ Dynamic Optimization and Differential Games*], John Wiley & Sons (2005).

[23] Nash, J., "Equlibrium points in n-person games," *Proceedings of the National Academy Sciences,* **36, No.1**, 48–49 (1950).

[24] Katic, I., Hojstrup, J., and Jensen, N., "A simple model for cluster efficiency," *Proc. of European Wind Energy Association Confererence and Exhibition*, 407–410 (1986).

[25] Bartl, J., [*Wake Measurement Behind an Array of Two Model Wind Turbines*], M.S. Thesis, Royal Institute of Technology, Stockholm, Sweden (2011).

[26] Boyd, S. and Vandenberghe, L., [*Convex Optimization*], Cambridge University Press (2011).